Cancer Cell
Article

JAK2/STAT5 Inhibition Circumvents Resistance to PI3K/mTOR Blockade: A Rationale for Cotargeting These Pathways in Metastatic Breast Cancer

Adrian Britschgi,[1] Rita Andraos,[2] Heike Brinkhaus,[1] Ina Klebba,[1] Vincent Romanet,[2] Urs Müller,[1] Masato Murakami,[2] Thomas Radimerski,[2] and Mohamed Bentires-Alj[1,*]
[1]Friedrich Miescher Institute for Biomedical Research, Basel, CH-4058, Switzerland
[2]Novartis Institutes for Biomedical Research, Disease Area Oncology, Basel, CH-4057, Switzerland
*Correspondence: bentires@fmi.ch
http://dx.doi.org/10.1016/j.ccr.2012.10.023

SUMMARY

Hyperactive PI3K/mTOR signaling is prevalent in human malignancies and its inhibition has potent antitumor consequences. Unfortunately, single-agent targeted cancer therapy is usually short-lived. We have discovered a JAK2/STAT5-evoked positive feedback loop that dampens the efficacy of PI3K/mTOR inhibition. Mechanistically, PI3K/mTOR inhibition increased IRS1-dependent activation of JAK2/STAT5 and secretion of IL-8 in several cell lines and primary breast tumors. Genetic or pharmacological inhibition of JAK2 abrogated this feedback loop and combined PI3K/mTOR and JAK2 inhibition synergistically reduced cancer cell number and tumor growth, decreased tumor seeding and metastasis, and also increased overall survival of the animals. Our results provide a rationale for combined targeting of the PI3K/mTOR and JAK2/STAT5 pathways in triple-negative breast cancer, a particularly aggressive and currently incurable disease.

INTRODUCTION

Detailed understanding of the genetic abnormalities that drive subsets of cancer has led to the development of highly specific inhibitors targeting key oncogenic pathways. The clinical efficacy and low toxicity of some of these mechanism-based therapies raised hopes for a new era in the treatment of cancer (Haber et al., 2011; Sellers, 2011). This is illustrated by several therapeutic successes, including imatinib in chronic myelogenous leukemia carrying the *BCR-ABL* fusion gene (O'Brien et al., 2003), and targeting V600E mutant B-RAF in metastatic melanoma (Flaherty et al., 2010). At the same time, it became evident that genetic and adaptive resistance are major obstacles in translating therapeutic efficacy into curative cancer therapy due to the evolutionary nature of cancer and the instable genome of some cancers. A thorough understanding of the "wiring diagram" of cancer cells and the mechanisms of resistance to targeted therapy is of paramount importance for designing multidrug combinations (Haber et al., 2011; Sellers, 2011).

The phosphatidylinositol 3-kinase (PI3K) signaling axis is vital for cell metabolism, proliferation, survival, and motility (Engelman et al., 2006). Class I PI3Ks phosphorylate phosphatidylinositol-4,5-bisphosphate and generate phosphatidylinositol-3,4,5-trisphosphate downstream of growth factor receptors and G protein-coupled receptors. This leads to activation of several kinases, including protein kinase B (PKB/AKT), mammalian target of rapamycin (mTOR), and p70 ribosomal protein S6 kinase (S6K) (Engelman et al., 2006). Studies in *Drosophila melanogaster* and in mammalian cells have revealed a PI3K regulatory negative feedback in which activation of S6K dampens IGF1-receptor (IGF-1R)/PI3K signaling via suppression of IRS1 (Harrington et al., 2004; Haruta et al., 2000; Radimerski et al., 2002).

The PI3K signaling cascade is one of the most frequently hyperactivated pathways in human cancer (Samuels et al., 2004). Not surprisingly, different classes of PI3K, AKT, and mTOR inhibitors have been developed and 26 compounds are presently in clinical trials (Engelman, 2009; Sheppard et al., 2012). Early results show limited efficacy of allosteric mTOR complex 1

Significance

The PI3K/mTOR pathway is very often subverted during tumorigenesis and contributes to numerous hallmarks of cancer. Twenty-six inhibitors of this pathway are currently in clinical trials. Using various cell lines and primary tumor models of triple-negative breast cancer, we have discovered that PI3K/mTOR inhibition elicits a positive feedback loop by activating JAK2/STAT5. This induces secretion of the pro-metastatic cytokine IL-8, which in turn feeds back into JAK2/STAT5, thereby completing the loop. Notably, inhibition of JAK2 abrogated this feedback, reduced tumor seeding and metastasis and increased overall survival of the animals. These data suggest IL-8 as a predictor of the efficacy of PI3K/mTOR inhibition and provide a rationale for combined inhibition of the PI3K/mTOR and JAK2/STAT5 pathways in triple-negative breast cancer.

(mTORC1) inhibition, most likely because it abrogates S6K-mediated negative feedback, leading to reactivation of PI3K/AKT signaling (O'Reilly et al., 2006). Similarly, allosteric AKT inhibition reactivates several RTKs that attenuate the beneficial effect of the inhibitor (Chandarlapaty et al., 2011). These studies stress the urgent need to identify mechanisms of resistance to PI3K pathway inhibition in order to rationally design optimal drug combinations.

The Janus family of kinases (JAKs) and their associated signal transducers and activators of transcription (STATs) also play a key role in cancer. Activation of JAKs/STATs stimulates cell proliferation, differentiation, migration, and survival (Harry et al., 2012). The JAK/STAT pathway is activated upon binding of hormones and cytokines (e.g., prolactin and interleukins) to their receptors. In neoplasia, the ligands are secreted by cancer cells and/or by cells from the tumor microenvironment (Bissell and Radisky, 2001). JAKs/STATs can also be activated by gain-of-function mutations like the JAK2 V617F mutation in myeloproliferative neoplasms, for which JAK2 inhibitors have shown promising activity (Harrison et al., 2012).

Given the many inhibitors of the PI3K pathway currently being evaluated, we sought to understand the effects of inhibiting this pathway on signaling in order to anticipate potential mechanisms of resistance. We assessed the effects of PI3K/mTOR inhibition in triple-negative breast cancer (TNBC), which is characterized by the absence of expression of estrogen and progesterone as well as ERBB2/HER2 receptors, is associated with a dismal prognosis, and still lacks effective targeted therapies (Hudis and Gianni, 2011).

RESULTS

PI3K/mTOR Inhibition Activates JAK2/STAT5

As PI3K/mTOR is a crucial oncogenic signaling node, its inhibition would be expected to activate compensatory mechanisms. To test this, we assessed the effects of inhibiting the PI3K/mTOR pathway in PTEN-deficient MDA-MB468 (MDA468) and RAS-mutated MDA-MB231 LM2 (MDA231 LM2) human breast cancer cells and in the mouse breast cancer line 4T-1. Single doses of BEZ235, a dual PI3K/mTOR inhibitor currently in clinical trials (Maira et al., 2008; Serra et al., 2008), were applied and the phosphorylation levels of several signaling proteins measured. BEZ235 reduced pAKT and completely blocked pS6 levels up to 20 hr in vitro and in vivo (Figure 1A; Figure S1A available online). Surprisingly, we also detected considerable upregulation of pJAK2 and pSTAT5, but not consistently of pSTAT3, after BEZ235 treatment (Figures 1A and S1A).

To elucidate which arm of the dual PI3K/mTOR inhibitor BEZ235 was responsible for the observed crosstalk to JAK2/STAT5, we applied the pan-PI3K inhibitor BKM120 and the mTORC1 inhibitor RAD001. Individual inhibition of either PI3K and mTORC1 upregulated pJAK2 and pSTAT5. Notably, although RAD001 readily activated JAK2/STAT5 after 4 hr treatment, BKM120 induced JAK2/STAT5 only after 8 hr (Figure S1B).

Both JAK1 and JAK2 signal to STAT5 and STAT3 depending on cell type and the receptor with which they are associated (Desrivières et al., 2006). Thus, we examined whether JAK1 and/or JAK2 are responsible for STAT5 activation upon PI3K/mTOR inhibition. siRNA depletion of each JAK isoform revealed that JAK2 activates STAT5 while JAK1 is upstream of STAT3 in our models (Figure 1B). Furthermore, siRNA depletion and inhibition of JAK2 by the JAK2-specific inhibitor NVP-BSK805 (Baffert et al., 2010) both counteracted the BEZ235-mediated upregulation of pSTAT5 (Figure 1C). As found in other models (Andraos et al., 2012), JAK2 inhibition by NVP-BSK805 efficiently blocked phosphorylation of STAT5 but did not reduce phosphorylation of JAK2.

Combined PI3K/mTOR and JAK2 Inhibition Induces Cell Death

Notably, we observed rapid recovery of pAKT after treatment with BEZ235 in all models, whereas pS6 remained inhibited (Figures 1A and S1A). We found that PHLPP, the phosphatase that targets Ser473 of AKT (Gao et al., 2005), was downregulated after 8 hr of BEZ235 treatment (Figure S2A). In addition, mTORC2 inhibition by siRNA-mediated depletion of RICTOR combined with BEZ235 treatment prevented the recovery of pAKT Ser473 (Figure S2B). As JAK2 is known to activate PI3K (Jin et al., 2008; Yamauchi et al., 1998), it was conceivable that BEZ235-induced JAK2 activation contributed to AKT reactivation. To test this, we examined whether combined inhibition of JAK2 and PI3K/mTOR prolongs inhibition of pAKT. Indeed, although blocking JAK2 alone did not impact on pAKT levels, the combination of BEZ235 and NVP-BSK805 prolonged pAKT suppression (Figure 2A).

To determine effects of blocking JAK2/STAT5 signaling on cell viability, we treated breast cancer lines with NVP-BSK805 or BEZ235 alone or in combination at concentrations that inhibit their respective targets. Although NVP-BSK805 alone had no impact on cell viability, it significantly decreased the number of living cells when combined with BEZ235. Combination of NVP-BSK805 and BEZ235 also significantly reduced colony formation capacity compared with DMSO or the single drug treatments (Figure 2B). Similar results were obtained with combinations of a doxycycline-inducible shRNA against JAK2 or siRNA-mediated depletion of STAT5A and B and BEZ235 treatment (Figure S2C).

To assess effects on cell death, we performed FACS analysis of propidium iodide- and/or AnnexinV-stained cells (Figures 2C, left panel, and S2D). Addition of NVP-BSK805 to BEZ235-treated cells resulted in a 25%–41% decrease in cells in S-phase and an ~1.8-fold increase in cells in sub-G1 (Figure S2D). Interestingly, cell death was not induced by individual treatments but increased significantly after combined inhibition of PI3K/mTOR and JAK2/STAT5 (Figure 2C, left panel). Immunoblotting revealed upregulation and increased electrophoretic mobility of the BH3-only protein BIM and, thus, its activation following treatment with NVP-BSK805 alone or in combination with BEZ235 (Figure 2C, right panel). Because BIM is inhibited by ERK1/2 (Ley et al., 2003), we assessed ERK1/2 phosphorylation levels in cells treated with BEZ235 and/or NVP-BSK805 but found no consistent changes in pERK1/2 (Figure S2E). It was reported previously that activation of BIM and downregulation of the pro-survival BCL2-family member MCL1 are both required for induction of cell death (Certo et al., 2006). In line with this, immunoblotting showed degradation of MCL1 only in cells treated with both BEZ235 and NVP-BSK805 (Figure 2C, right panel). Consistently, we found an increase in cleaved PARP only after combined BEZ235/NVP-BSK805 treatment (Figure 2C, right panel).

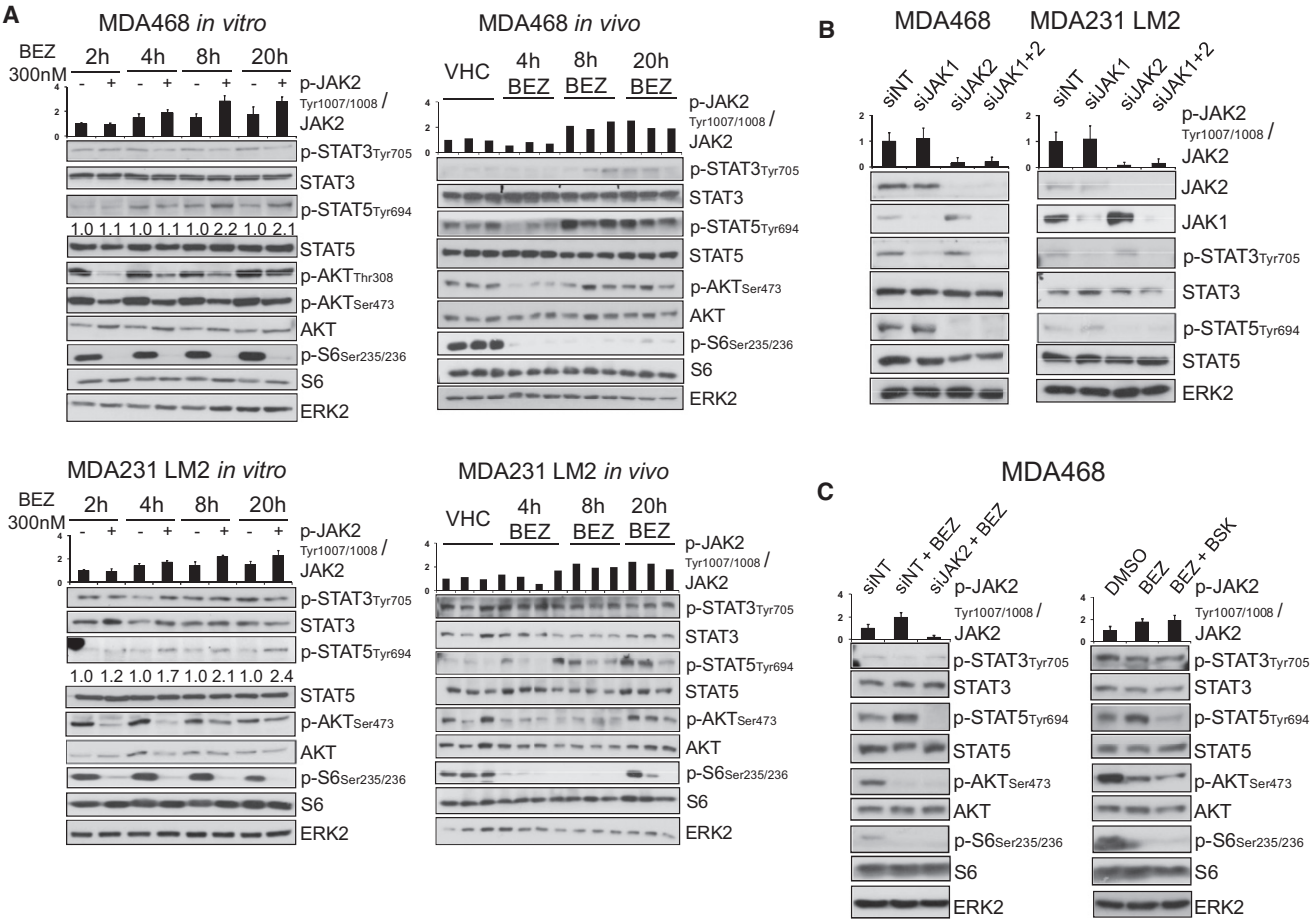

Figure 1. Dual PI3K/mTOR Inhibition by BEZ235 Activates JAK2/STAT5

(A) Immunoblots of lysates from breast cancer cells grown as monolayer cultures or as xenografts and treated with BEZ235 (BEZ). Mice bearing xenografts were treated with vehicle (VHC) or 30 mg/kg BEZ and dissected as indicated. The numbers indicate the ratios of pSTAT5/STAT5 as measured by densitometry. pJAK2 levels were measured in triplicate by ELISA and normalized to total JAK2 levels (y axis). ERK2 levels were used as a loading control.

(B) Immunoblots of lysates from breast cancer cells in which JAK2 and/or JAK1 were depleted by siRNA (siJAK). siNT, nontargeting control siRNA.

(C) Immunoblots of lysates from 8 hr BEZ-treated MDA468 cells in which JAK2/STAT5 signaling was blocked by JAK2 siRNA (left panel) or by the JAK2-specific inhibitor NVP-BSK805 (BSK) (right panel). ELISA data are means ± SD (n = 3).

See also Figure S1.

Given the involvement of the PI3K/AKT pathway in the regulation of several BH3-only proteins (Parcellier et al., 2008), we assessed the levels and activation states of BAD, BCL2, and BCL-XL. Both BCL2 and BCL-XL declined upon JAK2 inhibition or the combination treatment, whereas inactive pBAD decreased following PI3K/mTOR inhibition or the combination treatment (Figure 2C, right panel). These data indicate a pivotal involvement of decreased MCL1 in cell death induction by the combination of BEZ235 and NVP-BSK805.

Dual PI3K/mTOR Inhibition Triggers Secretion of IL-8

To determine whether the observed activation of JAK2/STAT5 upon BEZ235 treatment occurs via secretion of a soluble factor, we collected conditioned medium from cells treated for 20 hr with BEZ235, applied this to untreated cells, and lysed them 1 hr later. Medium supplemented with BEZ235 was used as a control. pJAK2 and pSTAT5 were both upregulated upon incubation with the conditioned medium compared with the control treatments, suggesting that a soluble factor mediated activation of JAK2/STAT5 (Figure 3A).

As JAKs are crucial transducers of cytokine signaling, we analyzed cytokine profiles after BEZ235 treatment, either in supernatants of cultured cells or lysates of tumor xenografts. Considerable changes in several cytokines were found, the most consistent being upregulation of IL-8 (Figure 3B).

To gain further insight into the kinetics of this response, we performed ELISA for IL-8 on supernatants of cells treated with BEZ235 (Figure 3C, left). A significant increase in IL-8 secretion was found after 20 hr of treatment. This secretion pattern was mirrored by upregulation of IL-8 mRNA, which suggested transcriptional regulation of the cytokine (Figure 3C, right).

To determine whether secreted IL-8 activated JAK2/STAT5 in breast cancer cells, we assessed whether these cells express its cognate receptors, CXCR1 and CXCR2. There was a 2.8- to 3-fold higher expression of CXCR1 than CXCR2 on both MDA468 and MDA231 LM2 cells (Figure S3A). Stimulation with cytokines

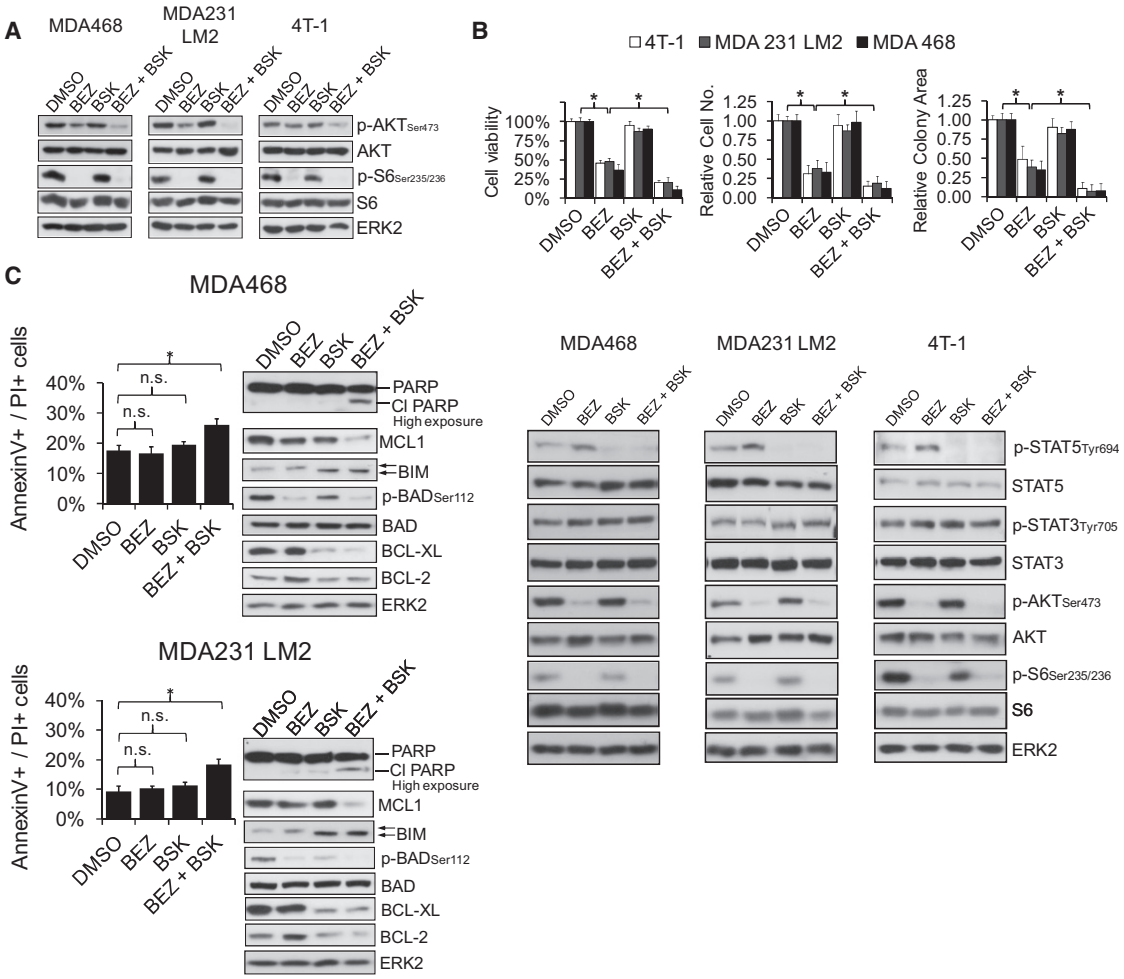

Figure 2. Cotargeting PI3K/mTOR and JAK2 Reduces Cell Viability

(A) Immunoblots of lysates of breast cancer cells after 20 hr of treatment with BEZ or BSK alone or in combination. DMSO, lysates of cells treated with 0.005% DMSO for 20 hr.

(B) Bar graphs showing the mean percentage of cell viability measured by the WST-1 assay (upper left) and by Trypan Blue cell counts (upper middle) of cell lines grown under 0.5% serum and treated with 300 nM BEZ and/or 350 nM BSK for 72 hr. Bar graph representing colony formation frequencies of cells treated as indicated (upper right). Immunoblots of lysates from the same cell lines after 8 hr of treatment as indicated are shown in the lower panel. Data are means ± SEM (n = 4, *p < 0.05).

(C) Bar graphs showing the mean percentage of apoptotic and dead cells after 48 hr of treatment as measured by FACS analysis of AnnexinV and PI stained cells treated with 300 nM BEZ and/or 350 nM BSK as indicated (left panel). Immunoblots of lysates from cells treated with 300 nM BEZ and/or 350 nM BSK for 24 hr (right panel). Data are means ± SEM (n = 5, *p < 0.05).

See also Figure S2.

known to activate JAK2/STAT5 in different cellular settings revealed strong activation of JAK2/STAT5 by IL-8 (Figure S3B).

Chemotherapy can induce senescence-associated secretion of cytokines, including IL-8 (Rodier and Campisi, 2011). We tested whether BEZ235 induces senescence by treating cells with the inhibitor for 5 days and then stained for β-galactosidase activity. We found that BEZ235 did not induce senescence in breast cancer cell lines (Figure S3C).

Activation of JAK2/STAT5/IL-8 Is Frequent in BEZ235-Insensitive TNBC Models

To assess the generality of our findings, we treated a panel of 18 breast cancer lines with BEZ235 and measured JAK2/STAT5 activation and IL-8 secretion. TNBC lines showed a higher baseline of pJAK2 and pSTAT5 than luminal cell lines and enhanced secretion of IL-8. Importantly, pJAK2, pSTAT5, and/or IL-8 secretion increased in 11 of the 18 lines upon BEZ235 treatment. Notably, the significant correlation found between BEZ235-triggered activation of JAK2 and IL-8 secretion strongly supports the generality of the crosstalk demonstrated between PI3K/mTOR and JAK2/STAT5/IL-8 in TNBC (Figure 3D; Table S1).

Our data suggested that activation of JAK2/STAT5 counteracts BEZ235-mediated reduction in cell viability (see Figures 2B and S2D). Therefore, we asked whether the upregulation of JAK2/STAT5/IL-8 upon BEZ235 treatment is correlated with

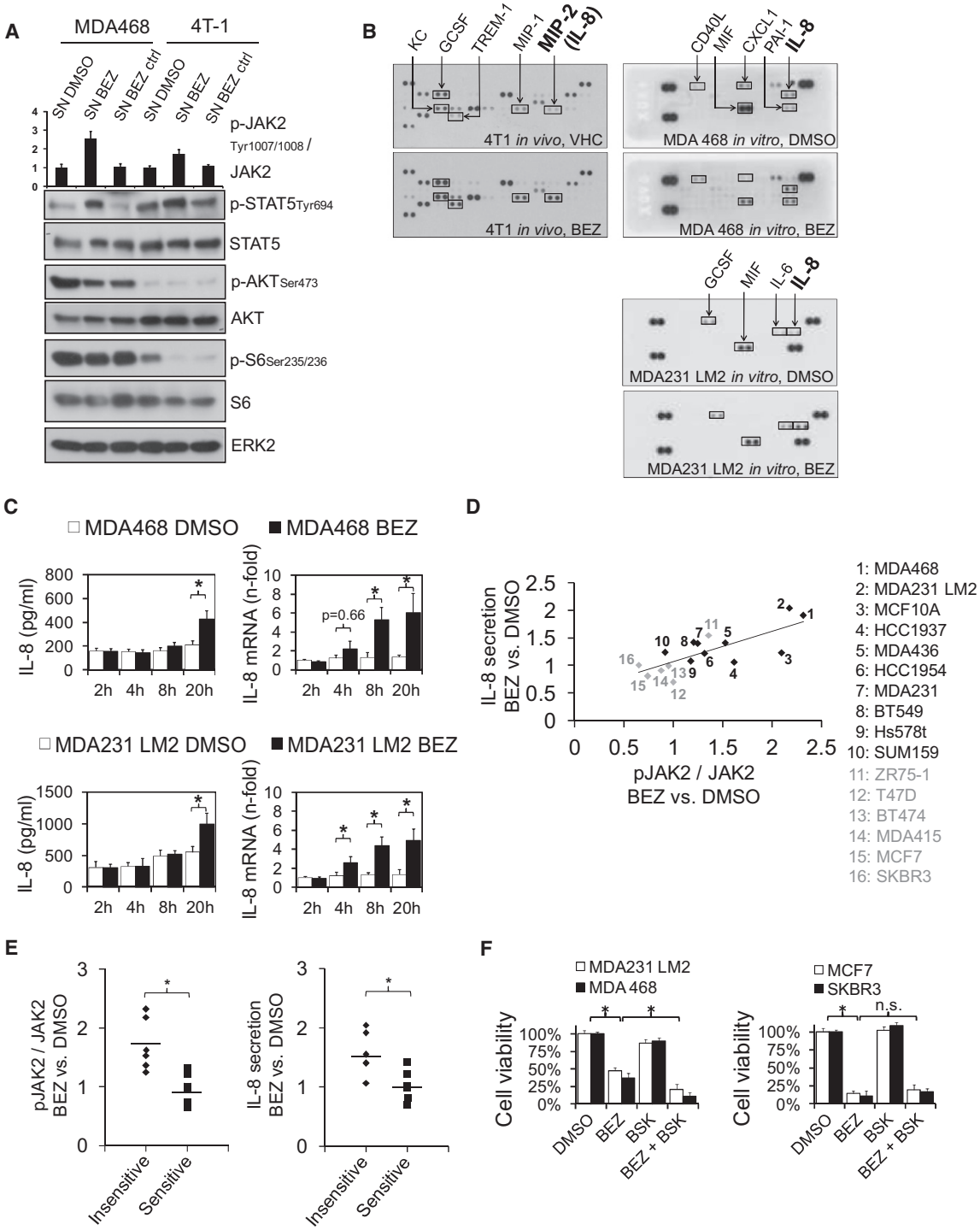

Figure 3. Dual PI3K/mTOR Inhibition Induces IL-8 Secretion in BEZ235-Insensitive Breast Cancer Cells

(A) Immunoblots of lysates from cells treated for 1 hr with conditioned media from cells treated with 300 nM BEZ for 20 hr. Lysates of cells treated with medium containing BEZ (SN BEZ ctrl) were used as a control for the BEZ present in the conditioned media. ELISA data are means ± SD (n = 3).

(B) Cytokine arrays showing expression of the indicated cytokines in supernatants of cells treated with 300 nM BEZ for 24 hr (upper panel) or in tumors from mice treated with 30 mg/kg BEZ for 10 days (lower panel). Mouse MIP2 is the functional homolog of human IL-8.

(C) Bar graphs showing the levels of IL-8 secretion (left panel) and mRNA (right panel) in cells treated with 300 nM BEZ as indicated. Levels of IL-8 were measured by ELISA and RT-qPCR and are shown as means ± SEM (n = 4, *p < 0.05).

(D) Scatter plot showing correlation in breast cancer lines between IL-8 secretion and the ratios of pJAK2/JAK2 upon BEZ treatment for 20 hr and 8 hr, respectively. Grey: luminal-like lines. Black: TNBC lines. Values from BEZ-treated relative to DMSO cells are shown (see also Table S1). Data are means of three independent experiments (n = 16, correlation = 0.77, p = 0.0006).

the sensitivity of cell lines to this inhibitor. Comparison of pJAK2 and IL-8 levels in 12 breast cancer cell lines to their reported sensitivity to BEZ235 (Brachmann et al., 2009) revealed higher activation of JAK2 and upregulation of IL-8 in BEZ235-insensitive than in sensitive lines (Figure 3E). Combined inhibition of PI3K/mTOR and JAK2 reduced the viability of BEZ235-insensitive lines further, underscoring the relevance of the crosstalk between the PI3K and JAK2/STAT5 pathways for the response to PI3K/mTOR inhibition (Figure 3F).

Biphasic Activation of JAK2/STAT5 upon PI3K/mTOR Inhibition

To test whether IL-8 is necessary and sufficient for activation of JAK2/STAT5, we blocked CXCR1, and thus IL-8 signaling, at different time points after BEZ235 treatment using a CXCR1-neutralizing antibody. As predicted, blocking CXCR1 reduced pFAK (Figure S4A) (Ginestier et al., 2010). More importantly, CXCR1 inhibition efficiently blocked the induction of pJAK2/pSTAT5 after 20 hr of BEZ235 treatment but, surprisingly, failed to prevent activation after only 8 hr (Figure 4A). Furthermore, we found that depletion of CXCR1 by siRNA did not affect BEZ235-induced upregulation of pJAK2/pSTAT5 after 8 hr of treatment, but abrogated it after 20 hr of treatment (Figures S4B and S4C). This suggests a biphasic activation of JAK2/STAT5 upon PI3K/mTOR inhibition, the first phase being IL-8/CXCR1-independent and the second being IL-8/CXCR1-dependent. This is in line with the increase in IL-8 secretion observed after 20 hr of BEZ235 treatment (Figure 3C).

These results raised the question of how JAK2 and STAT5 are activated at earlier time points of PI3K/mTOR inhibition. Epidermal growth factor receptor (EGFR) activates JAK2 in some models (Yamauchi et al., 1997) and, as EGFR has been shown to be activated upon PI3K/mTOR inhibition (Muranen et al., 2012), we tested whether EGFR is important for the activation of JAK2/STAT5 upon PI3K/mTOR blockade. Cells were treated for 8 hr with BEZ235 and/or the EGFR inhibitor AEE788 (Traxler et al., 2004). Although inhibition of EGFR indeed reduced pSTAT5 levels, it did not block the upregulation following BEZ235 treatment (Figure S4D).

Components of the insulin receptor (IR)/IGF-1R signaling pathways have been shown to interact with JAK/STAT (Gual et al., 1998; Le et al., 2002) and the same pathways are upregulated and activated upon mTOR (Haruta et al., 2000) and AKT inhibition (Chandarlapaty et al., 2011). Hence, there appears to be crosstalk between activation of the IR/IGF-1R pathways induced by AKT/mTOR inhibition and JAK2/STAT5. Indeed, IR and IGF-1R were upregulated and underwent increased phosphorylation upon BEZ235 treatment for 8 and 20 hr; IRS1 accumulated and showed increased phosphorylation after 2–20 hr of treatment (Figure 4B).

These data showed that accumulation of IRS1 preceded and possibly accounted for the first wave of pJAK2/pSTAT5 activation. Coimmunoprecipitation studies revealed association of both JAK2 and STAT5 with IRS1 in BEZ235- as well as DMSO-treated cells, but only weak association of JAK1 and STAT3 with IRS1 (Figure 4C). Our data thus showed that JAK2/STAT5 bind to IRS1 but not whether binding accounts for the first phase of BEZ235-induced pJAK2/pSTAT5. To address this question, we depleted IRS1 prior to BEZ235 treatment and found that this abrogated JAK2/STAT5 activation (Figure 4D, upper panel); thus, the first phase of JAK2/STAT5 activation appears to be IRS1-dependent.

Next, we examined whether the first phase of JAK2/STAT5 activation accounts for IL-8 upregulation and secretion by measuring IL-8 levels in the supernatant of cells expressing IRS1 siRNA and which were also treated with BEZ235. Depletion of IRS1 abrogated secretion of IL-8 upon BEZ235 treatment (Figure 4D, lower panel). In addition, knockdown of STAT5 or inhibition of JAK2 decreased BEZ235-evoked IL-8 transcription and secretion (Figures 4E and 4F), demonstrating that IL-8 upregulation is JAK2/STAT5-dependent.

Taken together, these data show that BEZ235-evoked activation of IR/IGF-1R/IRS1 triggered phosphorylation of JAK2/STAT5, which led to upregulation of IL-8 and induced the second phase of JAK2/STAT5 activation, thus completing a positive feedback loop.

Combined Inhibition of PI3K/mTOR and JAK2 Reduces Tumor Growth

That PI3K/mTOR inhibition triggers activation of JAK2/STAT5 and upregulation of IL-8 raises the possibility that this feedback loop could reduce the efficacy of PI3K/mTOR inhibitors in vivo. Using two independent orthotopic xenograft models and one orthotopic allograft model of breast cancer, we examined whether interfering with this feedback loop by inhibiting JAK2 affects the growth of tumors. Palpable tumors were treated with BEZ235 and/or inducible shRNA targeting JAK2, or with BEZ235 and/or NVP-BSK805. Single inhibition of JAK2 had no impact on tumor growth (Figures 5A–5D, left panels). However, tumor growth was reduced by treatment with BEZ235 and a synergistic reduction in tumor growth was seen when BEZ235 was combined with JAK2 inhibition (Figures 5A–5D, left panels). Tumor weight at the end of the treatments mirrored differences in tumor volume (Figures S5A and S5B). Notably, a synergistic effect was observed at lower doses of BEZ235 and NVP-BSK805 when combined than as individual treatments. Lower doses of the inhibitors were applied to avoid possible side-effects and potential drug-drug interaction of the combination. Indeed, there was no significant reduction in mouse body weight after any of the treatments (Figure S5C).

We then assessed the efficiency of PI3K/mTOR and JAK2 inhibition (Figures 5A–5D, right panels, and S5D). Both BEZ235 and NVP-BSK805 potently blocked their targets, as judged by the levels of pAKT/pS6 and pSTAT5, respectively. In addition, consistent with our previous results, pSTAT5 was strongly upregulated by BEZ235 treatment in all models, cleaved PARP

(E) Scatter plots showing breast cancer lines as in (D), depicted based on the ratios of pJAK2/JAK2 (left panel), the levels of secreted IL-8 (right panel) upon BEZ treatment, and sensitivity toward BEZ. The horizontal lines represent mean values (n = 3, *p < 0.05).
(F) Bar graphs showing the mean percentages of cell viability as measured by the WST-1 assay of two BEZ-insensitive lines (left panel) and two BEZ-sensitive lines (right panel) grown under 0.5% serum and treated with 300 nM BEZ and/or 350 nM BSK for 72 hr. Data are means ± SEM (n = 4, *p < 0.05).
See also Figure S3 and Table S1.

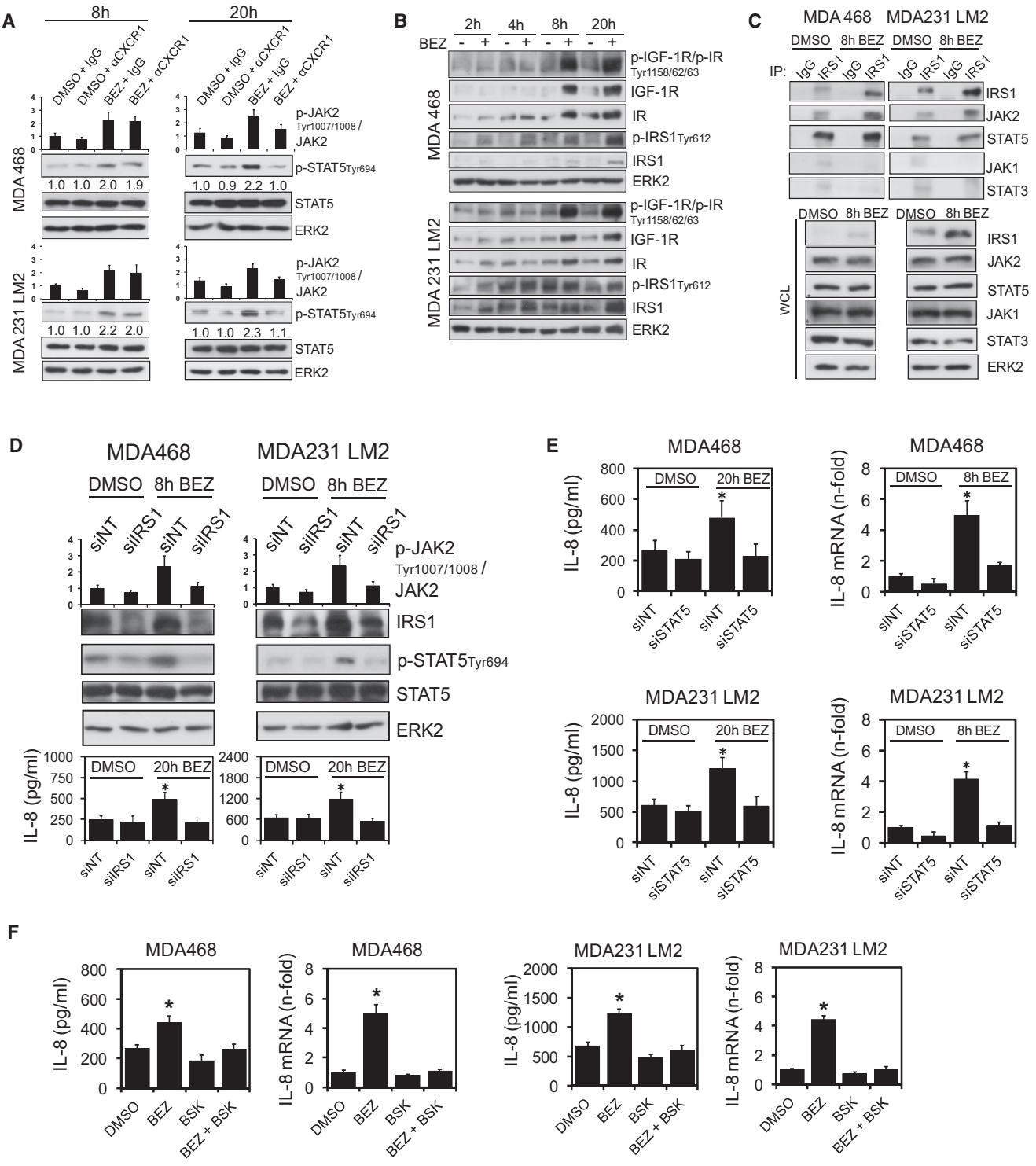

Figure 4. Cotargeting PI3K/mTOR Induces Biphasic Activation of JAK2/STAT5

(A) Immunoblots of lysates from cells treated with DMSO or 300 nM BEZ alone or in combination with IgG or a CXCR1-blocking antibody added 1 hr before lysis. The numbers indicate the ratios of pSTAT5/STAT5 as measured by densitometry. ELISA data are means ± SD (n = 3).

(B) Immunoblots of lysates from cells treated with 300 nM of BEZ as indicated.

(C) Immunoprecipitation (IP) and immunoblotting of lysates from cells treated with DMSO or 300 nM BEZ for 8 hr. WCL, whole cell lysates.

(D) Immunoblots of lysates from cells in which IRS1 was depleted by siRNA before treatment with DMSO or 300 nM BEZ for 8 hr. ELISA data are means ± SD (n = 3) (upper panel). Bar graphs showing the levels of IL-8 secretion upon treatment with 300 nM BEZ for 20 hr (lower panel). Levels of IL-8 were measured by ELISA and are shown as means ± SEM (n = 4, *p < 0.05).

increased in the combination treatment regime only, and proliferation declined in the BEZ235 and combination treatment groups (Figures 5A–5D, right panels, and S5E).

Combined Inhibition of PI3K/mTOR and JAK2 Reduces Metastasis

Metastasis is a multistep process that culminates with growth of tumor cells at distant sites. We analyzed the effects of targeting PI3K/mTOR alone or in combination with JAK2 inhibition on metastasis in mice injected with GFP-expressing MDA231 LM2 or 4T-1 metastatic cell lines. FACS analysis showed a slight reduction in the number of circulating GFP+ tumor cells (CTC) in the blood of mice following BEZ235 treatment, but a dramatic reduction after JAK2 inhibition or combined inhibition of PI3K/mTOR and JAK2 (Figure S5F). To test whether the reduction in CTCs was a consequence of reduced primary tumor volume, we calculated the CTC index upon PI3K/mTOR or JAK2 inhibition alone or in combination (Figure 5E). The CTC index was not affected by BEZ235 alone, but was significantly reduced by the combination of PI3K/mTOR and JAK2 inhibition or by JAK2 inhibition alone (Figure 5E). Next, we analyzed effects of the treatment on lung metastasis (Figure 5F). Importantly, although BEZ235 alone had no effect, the combination of BEZ235 and JAK2 inhibition or JAK2 inhibition alone reduced the metastatic index in all models (Figures 5G, 5H, S5G, and S5H).

To test whether this reduction in metastasis was due to cell-autonomous and/or noncell autonomous effects, we treated mice bearing tumors expressing shJAK2 either with vehicle or NVP-BSK805. No further reduction in the lung metastatic index was observed compared with single inhibition of JAK2 (Figure S5I). Thus, NVP-BSK805 mainly reduces metastatic burden in a cell-autonomous fashion.

Inhibition of JAK2 Blocks the BEZ235-Evoked IL-8/CXCR1 Pro-Metastatic Axis

To elucidate the mechanism underlying the reduction in metastasis observed upon combined PI3K/mTOR and JAK2 inhibition, we evaluated the impact of BEZ235 or NVP-BSK805 or their combination on IL-8 transcription and secretion in vitro and in vivo. Basal levels of active JAK2/STAT5 were higher in the highly metastatic breast cancer sublines 4T-1 and MDA231 LM2 than in the cognate poorly metastatic parental lines 168FARN and MDA231, respectively (Figure S6A). Consistently, the metastatic MDA231 LM2 cells exhibited stronger transcription and secretion of IL-8 (Figure S6B) and higher expression of the IL-8 surface receptor CXCR1 (Figure S6C) than the parental MDA231 cell line. Moreover, we found a correlation between IL-8 secretion, the triple-negative subtype and invasiveness in luminal and TNBC lines (Neve et al., 2006) (Figure S6D). We then compared CXCR1 expression levels in invasive, BEZ235-resistant cell lines and in noninvasive, BEZ235-sensitive cell lines. A striking correlation between CXCR1 expression and the invasive, BEZ235-resistant phenotype was observed, suggesting the involvement of CXCR1 signaling in invasion and adaptive resistance toward BEZ235 (Figure S6E; see also Figure 3E).

Given that IL-8 was induced by PI3K/mTOR inhibition and reduced by blockade of JAK2 in vitro (Figure 4F), we examined whether this was also the case in vivo. We found IL-8 to be elevated in tumors (Figure 6A) and in the plasma of BEZ235-treated mice (Figure 6B); this was reduced by inhibition of JAK2 or both JAK2 and PI3K/mTOR. To address the consequences of increased IL-8 secretion, we inhibited the IL-8 receptor in vitro using a CXCR1-blocking antibody and in vivo by Repertaxin, a noncompetitive allosteric CXCR1/2 inhibitor (Bertini et al., 2004). Combined inhibition of IL-8 and PI3K/mTOR reduced invasion as well as the CTC and metastatic indices. Notably, inhibition of IL-8 did not enhance the effects of JAK2 inhibition in these assays, further supporting roles for IL-8/CXCR1/JAK2 in invasion, tumor seeding and metastasis (Figures 6C–6E and S6F).

IL-8 and CXCR1 have been shown to be important for tumor-initiating cells (Ginestier et al., 2010). We confirmed this observation using limiting dilution transplantation of $CXCR1^+$ and $CXCR1^-$ cell populations (Figure S6G). FACS analysis of dissociated tumor cells, CTCs and lungs from vehicle-treated mice bearing xenografts revealed that only 3% of primary tumor cells were $CXCR1^+$ but CTCs were almost exclusively $CXCR1^+$ (96%). Furthermore, 20.5% of lung metastases cells expressed the receptor at high levels (Figure 6F). In the primary tumor, the $CXCR1^+$ population increased 1.9-fold upon PI3K/mTOR inhibition and decreased 2-fold upon inhibition of JAK2 alone or in combination with PI3K/mTOR inhibition (Figure 6G). Notably, JAK2 inhibition preferentially triggered cell death in the $CXCR1^+$ subpopulation (Figure 6H). Consistently, limiting dilution transplantation experiments revealed a decrease in tumor-initiating cell frequency upon JAK2 inhibition alone or in combination with PI3K/mTOR inhibition (Figures 6I and S6H).

Collectively, our data demonstrate that inhibition of the JAK2/STAT5/IL-8 positive feedback loop triggered by PI3K/mTOR blockade reduced tumor growth and seeding as well as lung metastasis due to its impact on the tumorigenic and metastatic $CXCR1^+$ subpopulation of cancer cells. This strongly suggests that the combination of PI3K and JAK2 inhibitors may be more effective in the neoadjuvant setting than either inhibitor alone.

PI3K/mTOR Inhibition Activates JAK2/STAT5/IL-8 in Primary Human Breast Tumors

We next assessed whether interfering with PI3K/mTOR in human primary breast tumors also triggered a JAK2/STAT5/IL-8 positive feedback loop. BEZ235 treatment of human primary TNBCs grown as xenografts increased pJAK2 and pSTAT5 (Figure 7A). Moreover, IL-8 in the tumors and in the plasma of the mice also increased upon treatment with BEZ235 (Figure 7B). These

(E) Bar graphs showing the levels of IL-8 secretion (left panel) and mRNA (right panel) upon treatment with 300 nM BEZ for 20 hr (left panel) or 8 hr (right panel). Levels of IL-8 were measured by ELISA and RT-qPCR, and are shown as means ± SEM (n = 4, *p < 0.05). For immunoblots of lysates from siSTAT5 depleted cells see Figure S2B.

(F) Bar graphs showing the levels of IL-8 secretion (left panel) and mRNA (right panel) upon treatment with 300 nM BEZ and/or 350 nM BSK for 20 hr (left panel) or 8 hr (right panel). Levels of IL-8 were measured by ELISA and RT-qPCR, and are shown as means ± SEM (n = 4, *p < 0.05).

See also Figure S4.

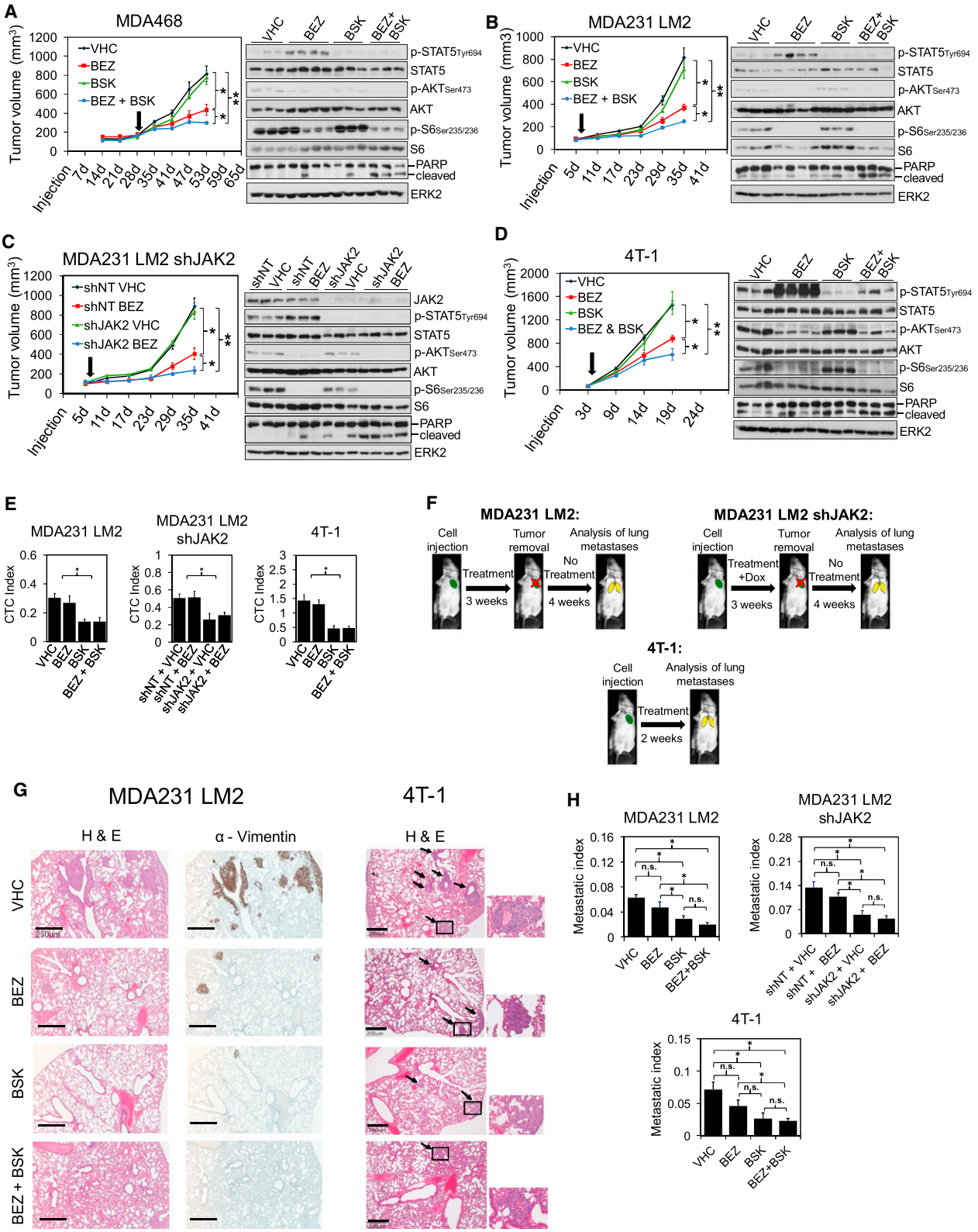

Figure 5. Cotargeting PI3K/mTOR and JAK2/STAT5 Reduces Primary Tumor Growth, Tumor Seeding, and Metastasis

(A–D) Growth curves of tumors and immunoblots of tumor lysates from mice treated with VHC, 30 mg/kg BEZ, 120 mg/kg BSK, or 25 mg/kg BEZ and 100 mg/kg BSK. In (C) JAK2 was depleted in tumors by doxycycline (dox) administration to induce expression of a JAK2-targeting shRNA (shJAK2). shNT, nontargeting shRNA. Injection refers to orthotopic cell injection and the arrows indicate initiation of treatment and/or administration of dox. Immunoblotting was performed on

data showed that the identified positive feedback loop mediated by PI3K/mTOR inhibition is also active in human primary breast tumors and suggest that targeting JAK2 in addition to PI3K/mTOR should block this resistance mechanism and enhance the efficacy of the inhibitors.

Combined PI3K/mTOR and JAK2 Inhibition Increases Survival in a Preclinical Setting

To leverage the mechanistic understanding gained from our experiments into a preclinical setting and to assess the therapeutic relevance of our findings, we performed survival studies using two different metastatic models. We treated tumor-bearing mice with BEZ235 and/or NVP-BSK805 and scored the time at which primary tumors reached 1 cm^3 (event-free survival) (Figure 8A). To mimic the neoadjuvant setting, we treated tumor-bearing mice with BEZ235 and/or NVP-BSK805, dissected the primary tumors, treated mice again, and then monitored them for signs of distress (overall survival) (Figure 8B). We found that BEZ235 treatment reduced primary tumor volume in both models and that JAK2 inhibition, although not affecting event-free survival, significantly enhanced overall survival. Most important, combination of BEZ235 and NVP-BSK805 enhanced preclinical benefit in terms of both event-free and overall survival of the animals.

DISCUSSION

Targeted anticancer drugs have greatly increased the hope of more effective and better tolerated therapies. Although some targeted therapies constitute a breakthrough and have changed the treatment landscape, in numerous cases they have not yet lived up to their promise, with the sobering realization that resistance can emerge within a few months (Engelman et al., 2008; Solit and Rosen, 2011). Delineation of these resistance mechanisms will pave the way for rationally designed and hopefully long-lasting combinations of targeted therapies. In the present study, we found that PI3K/mTOR inhibition elicits a positive feedback response in TNBC that leads to biphasic activation of JAK2/STAT5 and IL-8 secretion, thus dampening the response to the PI3K inhibitors. Our data suggest the following model (Figure 8C): in the untreated tumor (left), PI3K and mTOR are active and support survival and proliferation; JAK2/STAT5 signaling induces IL-8 production and contributes to metastasis. Upon PI3K/mTOR inhibition (middle), IRS1 as well as IGF-1R and IR accumulate and lead to the first wave of JAK2/STAT5 hyperactivation. JAK2/STAT5 activity in turn restores pAKT and blocks cell death, thereby offsetting the impact of BEZ235 on cell viability. JAK2/STAT5 activation also leads to an increase in IL-8 secretion, which activates the second wave of JAK2/STAT5 and completes the feedback loop. Moreover, IL-8 increases the relative number of $CXCR1^+$ cells. The efficacy of PI3K/mTOR inhibition can be improved dramatically by simultaneous JAK2 inhibition (right), which reduces the viability of $CXCR1^+$ tumor-initiating cells, the number of CTCs, and metastatic spread as well as increase the overall survival of the animals.

Identification of a Multimodal Mechanism of Resistance to PI3K/mTOR Inhibition

Mechanisms of resistance to targeted therapy often involve mutation of the target (Engelman and Jänne, 2008), reactivation of the targeted pathway (vertical resistance) (Chandarlapaty et al., 2011; Engelman et al., 2007), or activation of alternative survival pathways (horizontal resistance) (Turke et al., 2010). Activation of the PI3K pathway accounts for vertical and horizontal resistance to several targeted therapies, including inhibitors of EGFR, ERBB2, NOTCH, and MEK1 (Berns et al., 2007; Engelman et al., 2007; Palomero et al., 2007; Wee et al., 2009). But how does resistance to PI3K pathway inhibition occur? Notably, all reported mechanisms leading to escape from inhibition of this pathway comprise vertical resistance. Indeed, treatment with mTOR or AKT inhibitors may lead to reactivation of upstream components of the PI3K pathway (Chandarlapaty et al., 2011; Haruta et al., 2000; O'Reilly et al., 2006).

In the present study, we have uncovered a multimodal mechanism of resistance to targeting PI3K/mTOR. Biphasic activation of JAK2/STAT5 stifles the actions of PI3K/mTOR inhibition by reactivating AKT and increasing cell survival (vertical resistance), while at the same time increasing the systemic levels of the pro-metastatic cytokine IL-8 (horizontal resistance).

As expected, vertical cotargeting of the PI3K/mTOR pathway using dual inhibitors circumvented the IR/IGF-1R/IRS1-evoked reactivation of PI3K arising after mTOR inhibition, which most likely accounts for the limited success of rapalogs as single-agent anticancer therapies. Nevertheless, although dual PI3K/mTOR inhibition reduces reactivation of PI3K, the IR/IGF-1R/IRS1 axis remains active. The consequences of the sustained activity of this axis on other pathways and on the sensitivity to dual PI3K/mTOR inhibitors remain ill-defined. Our findings that PI3K/mTOR inhibition-mediated reactivation of

tumors harvested after 14 days of treatment for MDA468, 10 days of treatment for MDA231 LM2, and 6 days of treatment for 4T-1. Results are mean tumor volume ± SEM (three independent experiments, total n = 4–8, *p < 0.05, **p < 0.01).
(E) Bar graphs showing the circulating tumor cell (CTC) index. The number of CTCs was measured by FACS analysis of GFP+ cells in tail vein blood performed 21 days (MDA231 LM2) or 5 days (4T-1) after initiation of the treatment as in (B)–(D). The CTC index was calculated by dividing the total number of GFP+ CTCs per 100 μl peripheral blood by tumor volume. Data represent the means ± SEM (for MDA231 LM2 shJAK2 in two independent experiments, total of n = 4 mice, and for the other models in three independent experiments, with a total n = 7 mice; *p < 0.05).
(F) Drawings of the experimental setup.
(G) Representative IHC pictures of lungs from VHC-, BEZ-, BSK- and BEZ/BSK-treated animals. Left panel: H&E- (left) and Vimentin-(right) stained lungs from MDA231 LM2-bearing animals, treated as described in (B) and (F). Scale bar represents 250 μm. Right panel: H&E-stained lungs from 4T-1-bearing animals, treated as described in (D) and (F). Arrows indicate metastases; the images to the right are magnifications of single metastatic foci. Scale bar represents 200 μm.
(H) Bar graphs showing the metastatic index of mice treated as in (B–D) calculated by dividing the total number of visible lung metastases nodules by tumor volume. Data are means ± SEM (for MDA231 LM2 shJAK2 from two independent experiments, total n = 4, for the other models from three independent experiments, total n = 10, *p < 0.05).
See also Figure S5.

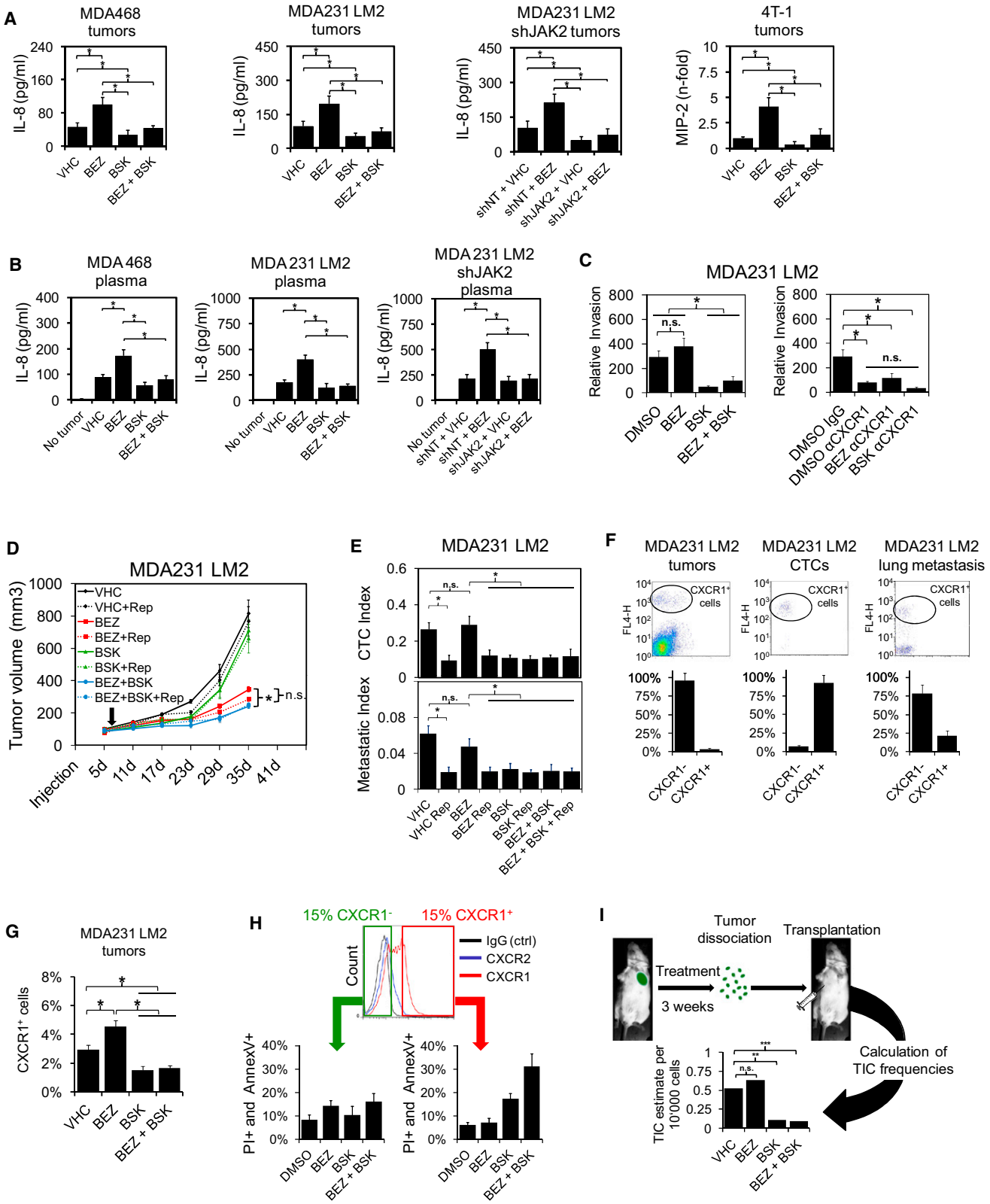

Figure 6. PI3K/mTOR Inhibition Increases, whereas JAK2 Inhibition Blocks IL-8 Secretion and Reduces the Tumor-Initiating CXCR1$^+$ Subpopulation

(A) Bar graphs showing IL-8 levels measured by ELISA (left and middle panels) or quantification of dots of cytokine arrays (right panel) from tumors of mice treated as in Figures 5A–5D. Data are means ± SEM (n = 3–8, *p < 0.05).

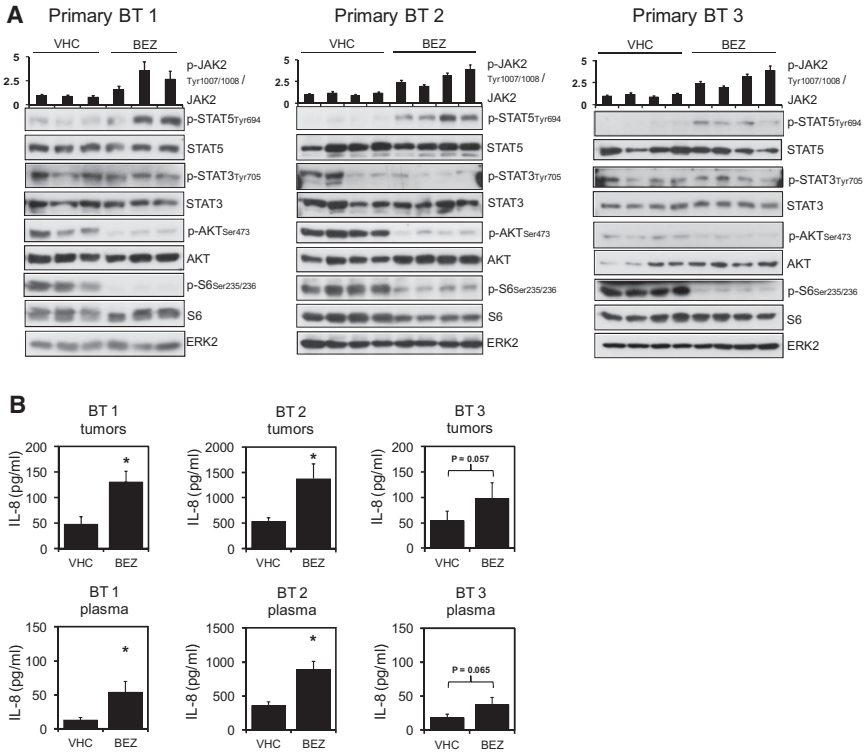

Figure 7. BEZ235 Treatment Activates JAK2/STAT5 and IL-8 Secretion in Primary Human TNBC Xenografts

(A) Immunoblots of lysates from primary TNBC xenografts treated for 4 days with 30 mg/kg BEZ or VHC. ELISA data are means ± SD (n = 3).

(B) Bar graphs showing IL-8 levels measured by ELISA in the dissected tumors from or in the plasma of mice at day 3 of treatment with 30 mg/kg BEZ or VHC. Data are means ± SEM (n = 3–4, *p < 0.05).

IR/IGF-1R/IRS1 induces a first wave of active JAK2/STAT5, which in turn contributes to rephosphorylation of AKT, shed light on this question. We further found that BEZ235 reduces the expression of the AKT Ser473 phosphatase PHLPP and that it inefficiently targets the mTORC2 complex. Genetic inhibition of mTORC2 blocked the recovery of pS473 AKT upon treatment with BEZ235, consistent with previous studies showing that inhibition of S6K-induced mTORC2/AKT (Dibble et al., 2009). These different feedback mechanisms may explain the limited efficacy of dual PI3K/mTOR inhibition in some cancer models. These results and our observation that individual PI3K or mTOR inhibition also causes JAK2/STAT5 activation raise the possibility that other inhibitors of the PI3K pathway may elicit similar crosstalk.

Cotargeting PI3K/mTOR and JAK2 Increases Cell Death and Reduces Tumor Growth

The PI3K and JAK2 pathways activate the prosurvival protein MCL1 and suppress the pro-apoptotic protein BIM at the transcriptional and posttranslational levels (Ewings et al., 2007; Opferman, 2006). We found that combined inhibition of PI3K/mTOR and JAK2 activates BIM and concomitantly downregulates MCL1, causing an increase in apoptosis. Notably, this latter effect was not observed upon single inhibition of PI3K/mTOR or JAK2/STAT5, suggesting that activation of either pathway prevents cell death. Combined PI3K and MEK inhibition similarly decreased MCL1 and increased BIM, thereby triggering cell death in EGFR mutant lung cancer (Faber et al., 2009). The moderate levels of cell death detected upon combined PI3K/mTOR and JAK2 inhibition, both in vitro and in vivo, can be explained by the fact that cell death was mainly induced in the small subpopulation of CXCR1$^+$ tumor-initiating cells.

Genetic depletion of JAK2 after overt tumor development was shown to have no effect on tumor growth (Sakamoto et al., 2009). Similarly, we found no effect of single JAK2 inhibition on tumor growth. However, (Hedvat et al., 2009; Xin et al., 2011) showed that a different JAK inhibitor reduced primary tumor growth of xenografts of MDA468 and 4T-1, two cell lines that we also

(B) Bar graphs showing IL-8 levels measured by ELISA in plasma of mice bearing tumors treated as in Figures 5A–5C. Data are means ± SEM (n = 4, *p < 0.05).

(C) Bar graphs showing relative invasion of MDA231 LM2 cells seeded on Matrigel-coated Boyden chambers and treated with 300 nM BEZ, 350 nM BSK and/or CXCR1 blocking antibody. Invasion was assessed after 48 hr. Data represent relative invasion values normalized to cell number and are means ± SEM (n = 4, *p < 0.05).

(D) Growth curves of tumors from mice treated with VHC, 30 mg/kg BEZ, 120 mg/kg BSK, 20 mg/kg Repertaxin (Rep), or 25 mg/kg BEZ, 100 mg/kg BSK and 20 mg/kg Rep. Injection refers to orthotopic cell injection and the arrow indicates initiation of treatment. Data are mean tumor volume ± SEM (n = 4–8, *p < 0.05).

(E) Bar graphs showing CTC (upper panel) and lung metastatic (lower panel) indices of mice treated as in Figure 5F. Rep was administered at 20 mg/kg. Data are means ± SEM (n = 3–4, *p < 0.05).

(F) Upper: representative images of FACS dot plots of CXCR1-stained tumors, CTCs and lungs. Lower: bar graphs showing the percentage of CXCR1$^+$ cells. Data are means ± SEM (n = 6).

(G) Bar graph showing percentages of CXCR1$^+$ cells in MDA231 LM2 tumors of mice treated as in Figure 5B. Data are means ± SEM (n = 4–6, *p < 0.05).

(H) Representative dot plot of FACS analyses performed on CXCR1- (upper panel), AnnexinV-, and PI-stained (lower panel) MDA231 LM2 cells treated with inhibitors as in Figure 2C. Bar graphs show the mean percentages of apoptotic and dead cells after 48 hr of treatment. Data are means ± SEM (n = 4, *p < 0.05).

(I) Upper: drawing of the experimental setup. Mice bearing MDA231 LM2 tumors were treated as in Figure 5B. The tumors were dissected, dissociated, and retransplanted at different dilutions. Cell viability prior to retransplantation was analyzed by PI-FACS staining and was found to be equal in all treatment groups (data not shown). Lower: bar graph showing the TIC frequencies after treatment as in Figure 5B. Data are mean estimates from three independent experiments, total n = 7 mice, *p < 0.05, ***p < 0.0001.

See also Figure S6.

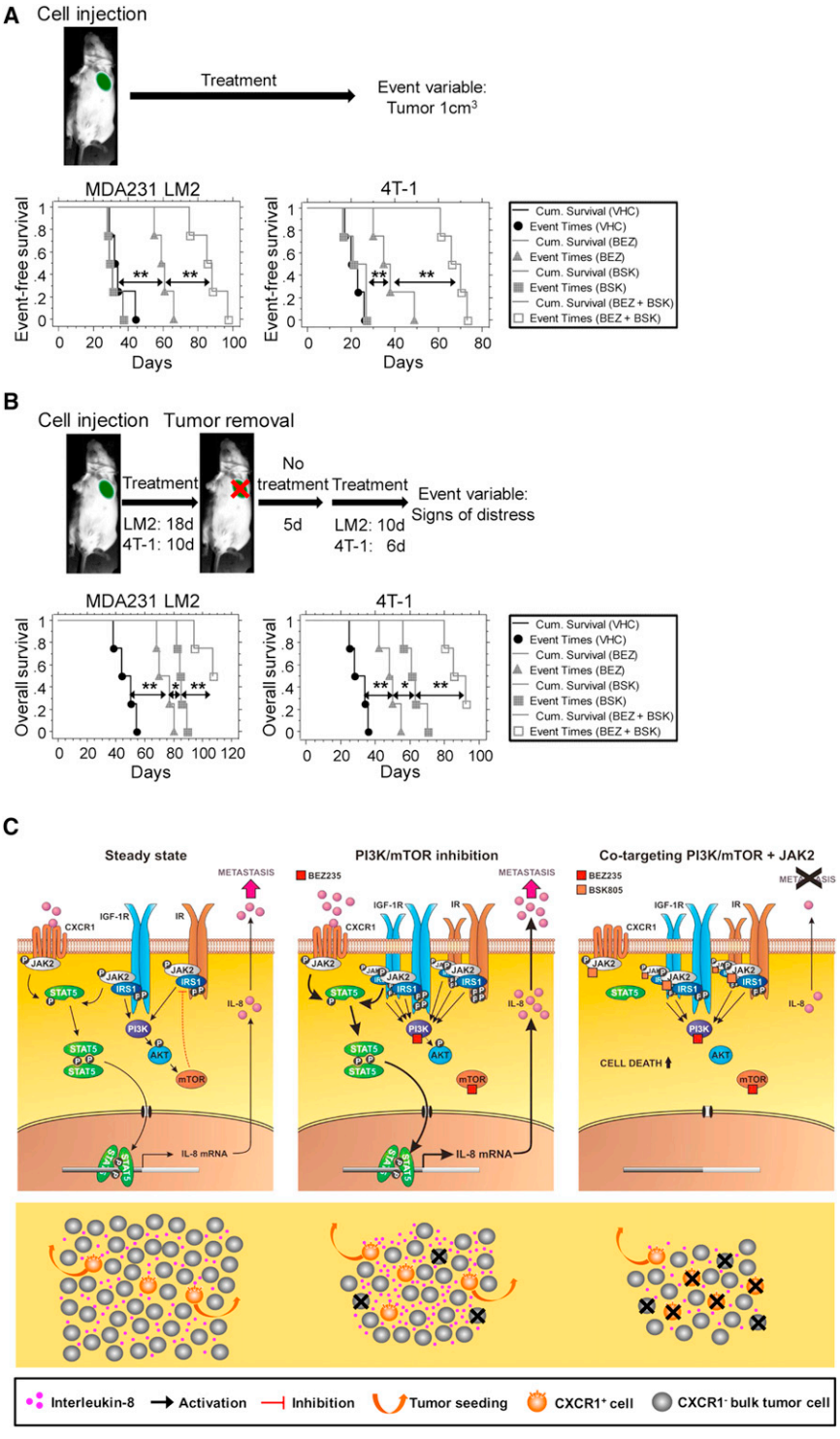

Figure 8. Cotargeting PI3K/mTOR and JAK2 Increases Event-Free and Overall Survival in Two Models of Metastatic Breast Cancer

(A) Upper: drawing of the experimental setup. Lower: Kaplan-Meier survival curves of MDA231 LM2 (left) and 4T-1 (right) tumor-bearing mice treated with BEZ and/or BSK as in Figures 5B and 5D. An event was scored when a tumor reached 1 cm^3 (n = 4, *p < 0.05, **p < 0.01).

(B) Upper: drawing of the experimental setup. Lower: Kaplan-Meier survival curves of MDA231 LM2 (left) and 4T-1 (right) tumor-bearing mice treated with BEZ and/or BSK as in Figures 5B and 5D. An event was scored when a mouse showed any sign of distress; (n = 4, *p < 0.05, **p < 0.01).

(C) Schematics illustrating the identified positive feedback loop triggered by inhibition of PI3K/mTOR and offset by JAK2/STAT5 inhibition. Upper: effects of PI3K/mTOR inhibition and/or JAK2 inhibition at the cellular level. Lower: effects of PI3K/mTOR and/or JAK2 inhibition at the tumor level.

used in the present study. This inhibitor (Hedvat et al., 2009) displayed a spectrum of JAK kinase selectivity different to NVP-BSK805, which is biased toward JAK2 within the JAK family (Baffert et al., 2010). Different inhibitors also display divergent spectra of overall kinase selectivity, which may also account for some of the tumor growth effects observed by (Hedvat et al., 2009). Of note, the focus of some of the other studies has been on oncogenic STAT3 signaling in breast cancer models (Hedvat et al., 2009; Marotta et al., 2011), whereas our present work has revealed an important role for JAK2/STAT5 signaling. RNAi experiments in our models showed that JAK2 is required for STAT5 phosphorylation, whereas JAK1 predominantly signals to STAT3. Hence, dual JAK1/2 inhibitors may have additional antitumor effects due to suppression of both STAT3 and STAT5 phosphorylation.

Inhibition of PI3K/mTOR and JAK2 or JAK2 Alone Reduces Metastasis and Increases Overall Survival

Consistent with the multimodal nature of the identified feedback, cotargeting PI3K/mTOR and JAK2/STAT5 also reduced tumor seeding and metastasis. These effects can be explained by the fact that targeting JAK2 abrogated this feedback loop, decreasing STAT5 activation and IL-8 transcription and secretion, which culminated in death of the $CXCR1^+$ cells. The observation that $CXCR1^+$ cells were a minor subpopulation in the primary tumor but constitute the majority of CTCs and ~20% of lung metastases raises the intriguing possibility that CXCR1 and its associated downstream signaling are crucial for intravasation and/or survival of the cells in the periphery, but less critical once cells have reached the metastatic site. Consistently, IL-8 inhibition alone or in combination with PI3K/mTOR inhibition reduced tumor seeding and metastasis. Indeed, IL-8 has been shown to play crucial roles

in the stimulation of tumor-initiating cells, invasion, and metastasis (Charafe-Jauffret et al., 2009; Ginestier et al., 2010; Waugh and Wilson, 2008), and a role for JAK2 in cells with the cancer stem cell phenotype has also been suggested (Marotta et al., 2011).

To gain insights into a potential clinical benefit of combined inhibition of PI3K/mTOR and JAK2, we performed survival studies in a preclinical setting. We found that single JAK2 inhibition increased overall survival, while having no benefit on event-free survival. Notably, combination of BEZ235 and NVP-BSK805 increased both event-free and overall survival of animals. Our findings potentially have direct clinical implications, given that 26 PI3K pathway inhibitors are currently undergoing clinical evaluation (Sheppard et al., 2012). These results urge assessment of the activation of the JAK2/STAT5/IL-8 positive feedback loop before therapy and/or upon PI3K inhibition, and the testing of the efficacy of cotargeting PI3K/mTOR and JAK2 in TNBC and other cancers.

EXPERIMENTAL PROCEDURES

Compounds

BEZ235, NVP-BSK805, NVP-BKM120, and RAD001 were from Novartis (Basel, Switzerland). Repertaxin L-lysine salt was obtained from WuXi AppTec (Shanghai, China). Daunorubicin was obtained from Sigma Aldrich. Compounds were prepared as 10 mM stock solutions in DMSO and stored protected from light at −20°C. NVP-BSK805 was freshly formulated in NMP/PEG300/Solutol HS15 (5%/80%/15%) and BEZ235 in NMP/PEG300 (10%/90%), and both were administered to mice by oral gavage at 10 ml/kg. Repertaxin was freshly formulated in PBS and administered subcutaneously at 20 mg/kg.

Primary Human Breast Tumors

Primary breast cancer specimens were obtained from the consented patients: two specimens were provided by the Cooperative Human tissue Network which is funded by the National Cancer institute, and one was obtained at and approved by the board of the Saint-Louis Clinic (France). All studies were approved by the Ethikkommission beider Basel.

Animal Experiments

SCID/beige, SCID/NOD, and Balb/c mice (Jackson Laboratories) were used in compliance with the Swiss laws on animal welfare and the animal protocols were approved by the Swiss Cantonal Veterinary Office of Basel. For orthotopic engraftment of breast cancer cell lines, 1×10^6 MDA468, 1×10^6 MDA231 LM2, and 0.5×10^6 4T-1 or 4T-1-GFP cells were suspended in a 100 μl mixture of Basement Membrane Matrix Phenol Red-free (BD Biosciences) and PBS 1:1 and injected into mouse mammary gland. Primary breast tumors were cut into 1 mm^3 pieces and transplanted into mouse mammary gland. Tumor-bearing mice were randomized based on tumor volume prior to the initiation of treatment, which started when average tumor volume was at least 100 mm^3. BEZ235 and NVP-BSK805 were given orally on each of 6 consecutive days followed by 1 day without the drug; Repertaxin was administered daily. Expression of shRNAs was induced by adding doxycycline in the drinking water (2 g/l in a 5% sucrose solution), which was refreshed every 48 hr. Tumors were measured every 3–4 days and tumor volumes calculated by the formula 0.5 × (larger diameter) × (smaller diameter)^2. End point tumor sizes were analyzed for synergism using the formula AB/C < A/C × B/C, where C is tumor volume VHC, A is tumor volume compound 1, B is tumor volume compound 2, and AB is tumor volume combination (Clarke, 1997). For survival studies, animals were sacrificed when tumors reached 1 cm^3 or when they showed any signs of distress (e.g., breathing disorders, weight loss, or immobility).

Statistical Analysis

Each value reported represents the mean ± SEM of at least three independent experiments. Data were tested for normal distribution and Student's t test, ANOVAs, or nonparametric Mann-Whitney U/Wilcoxon tests were applied. To account for multiple comparisons, Tukey HSD and Wilcoxon tests were performed. StatView 5.0.1 was used for Kaplan-Meier survival analysis and log rank Mantel-Cox tests were applied to test statistical significance (SAS). Programs JMP4 and JMP9 were used for all other statistical tests (SAS). The p values < 0.05 were considered to be statistically significant.

SUPPLEMENTAL INFORMATION

Supplemental Information includes six figures, one table, and Supplemental Experimental Procedures and can be found with this article online at http://dx.doi.org/10.1016/j.ccr.2012.10.023.

ACKNOWLEDGMENTS

We thank N. Hynes (FMI) for providing the 4T-1 and 168FARN cells and J. Massagué (MSKCC) and C. Kuperwasser (Tufts University) for providing the MDAMB 231 LM2 and SUM159 cells, respectively. We are grateful to W. Sellers (Novartis, ONC) for helpful discussions, M. Maira and C. Fritsch (Novartis, ONC) for supplying BEZ235 and BKM120, and H. Gao and F. Baffert (Novartis, ONC) and Y. Kuhn and C. Peters (Saint-Louis Clinic) for providing primary tumors. Tissue samples were provided by the Cooperative Human Tissue Network, which is funded by the National Cancer Institute. Other investigators may have received specimens from the same subjects. Thanks to H. Kohler, M. Stadler, R. Thierry, and S. Bourke (FMI) for help with data analysis and to further members of the Bentires-Alj lab for discussions. Research in the lab of M.B-A. is supported by the Novartis Research Foundation and the European Research Council. R.A., V.R., M.M., and T.R. are full-time employees of Novartis Pharma AG.

Received: June 7, 2012
Revised: October 8, 2012
Accepted: October 31, 2012
Published: December 10, 2012

REFERENCES

Andraos, R., Qian, Z., Bonenfant, D.b., Rubert, J.l., Vangrevelinghe, E., Scheufler, C., Marque, F., Régnier, C.H., De Pover, A., Ryckelynck, H., et al. (2012). Modulation of activation-loop phosphorylation by JAK inhibitors is binding mode dependent. Cancer Discov. *2*, 512–523.

Baffert, F., Régnier, C.H., De Pover, A., Pissot-Soldermann, C., Tavares, G.A., Blasco, F., Brueggen, J., Chène, P., Drueckes, P., Erdmann, D., et al. (2010). Potent and selective inhibition of polycythemia by the quinoxaline JAK2 inhibitor NVP-BSK805. Mol. Cancer Ther. *9*, 1945–1955.

Berns, K., Horlings, H.M., Hennessy, B.T., Madiredjo, M., Hijmans, E.M., Beelen, K., Linn, S.C., Gonzalez-Angulo, A.M., Stemke-Hale, K., Hauptmann, M., et al. (2007). A functional genetic approach identifies the PI3K pathway as a major determinant of trastuzumab resistance in breast cancer. Cancer Cell *12*, 395–402.

Bertini, R., Allegretti, M., Bizzarri, C., Moriconi, A., Locati, M., Zampella, G., Cervellera, M.N., Di Cioccio, V., Cesta, M.C., Galliera, E., et al. (2004). Noncompetitive allosteric inhibitors of the inflammatory chemokine receptors CXCR1 and CXCR2: prevention of reperfusion injury. Proc. Natl. Acad. Sci. USA *101*, 11791–11796.

Bissell, M.J., and Radisky, D. (2001). Putting tumours in context. Nat. Rev. Cancer *1*, 46–54.

Brachmann, S.M., Hofmann, I., Schnell, C., Fritsch, C., Wee, S., Lane, H., Wang, S., Garcia-Echeverria, C., and Maira, S.M. (2009). Specific apoptosis induction by the dual PI3K/mTor inhibitor NVP-BEZ235 in HER2 amplified and PIK3CA mutant breast cancer cells. Proc. Natl. Acad. Sci. USA *106*, 22299–22304.

Certo, M., Del Gaizo Moore, V., Nishino, M., Wei, G., Korsmeyer, S., Armstrong, S.A., and Letai, A. (2006). Mitochondria primed by death signals determine cellular addiction to antiapoptotic BCL-2 family members. Cancer Cell *9*, 351–365.

Chandarlapaty, S., Sawai, A., Scaltriti, M., Rodrik-Outmezguine, V., Grbovic-Huezo, O., Serra, V., Majumder, P.K., Baselga, J., and Rosen, N. (2011). AKT inhibition relieves feedback suppression of receptor tyrosine kinase expression and activity. Cancer Cell *19*, 58–71.

Charafe-Jauffret, E., Ginestier, C., Iovino, F., Wicinski, J., Cervera, N., Finetti, P., Hur, M.H., Diebel, M.E., Monville, F., Dutcher, J., et al. (2009). Breast cancer cell lines contain functional cancer stem cells with metastatic capacity and a distinct molecular signature. Cancer Res. *69*, 1302–1313.

Clarke, R. (1997). Issues in experimental design and endpoint analysis in the study of experimental cytotoxic agents in vivo in breast cancer and other models. Breast Cancer Res. Treat. *46*, 255–278.

Desrivières, S., Kunz, C., Barash, I., Vafaizadeh, V., Borghouts, C., and Groner, B. (2006). The biological functions of the versatile transcription factors STAT3 and STAT5 and new strategies for their targeted inhibition. J. Mammary Gland Biol. Neoplasia *11*, 75–87.

Dibble, C.C., Asara, J.M., and Manning, B.D. (2009). Characterization of Rictor phosphorylation sites reveals direct regulation of mTOR complex 2 by S6K1. Mol. Cell. Biol. *29*, 5657–5670.

Engelman, J.A. (2009). Targeting PI3K signalling in cancer: opportunities, challenges and limitations. Nat. Rev. Cancer *9*, 550–562.

Engelman, J.A., and Jänne, P.A. (2008). Mechanisms of acquired resistance to epidermal growth factor receptor tyrosine kinase inhibitors in non-small cell lung cancer. Clin. Cancer Res. *14*, 2895–2899.

Engelman, J.A., Luo, J., and Cantley, L.C. (2006). The evolution of phosphatidylinositol 3-kinases as regulators of growth and metabolism. Nat. Rev. Genet. *7*, 606–619.

Engelman, J.A., Zejnullahu, K., Mitsudomi, T., Song, Y.C., Hyland, C., Park, J.O., Lindeman, N., Gale, C.M., Zhao, X.J., Christensen, J., et al. (2007). MET amplification leads to gefitinib resistance in lung cancer by activating ERBB3 signaling. Science *316*, 1039–1043.

Engelman, J.A., Chen, L., Tan, X., Crosby, K., Guimaraes, A.R., Upadhyay, R., Maira, M., McNamara, K., Perera, S.A., Song, Y., et al. (2008). Effective use of PI3K and MEK inhibitors to treat mutant Kras G12D and PIK3CA H1047R murine lung cancers. Nat. Med. *14*, 1351–1356.

Ewings, K.E., Hadfield-Moorhouse, K., Wiggins, C.M., Wickenden, J.A., Balmanno, K., Gilley, R., Degenhardt, K., White, E., and Cook, S.J. (2007). ERK1/2-dependent phosphorylation of BimEL promotes its rapid dissociation from Mcl-1 and Bcl-xL. EMBO J. *26*, 2856–2867.

Faber, A.C., Li, D., Song, Y., Liang, M.C., Yeap, B.Y., Bronson, R.T., Lifshits, E., Chen, Z., Maira, S.M., García-Echeverría, C., et al. (2009). Differential induction of apoptosis in HER2 and EGFR addicted cancers following PI3K inhibition. Proc. Natl. Acad. Sci. USA *106*, 19503–19508.

Flaherty, K.T., Puzanov, I., Kim, K.B., Ribas, A., McArthur, G.A., Sosman, J.A., O'Dwyer, P.J., Lee, R.J., Grippo, J.F., Nolop, K., and Chapman, P.B. (2010). Inhibition of mutated, activated BRAF in metastatic melanoma. N. Engl. J. Med. *363*, 809–819.

Gao, T., Furnari, F., and Newton, A.C. (2005). PHLPP: a phosphatase that directly dephosphorylates Akt, promotes apoptosis, and suppresses tumor growth. Mol. Cell *18*, 13–24.

Ginestier, C., Liu, S., Diebel, M.E., Korkaya, H., Luo, M., Brown, M., Wicinski, J., Cabaud, O., Charafe-Jauffret, E., Birnbaum, D., et al. (2010). CXCR1 blockade selectively targets human breast cancer stem cells in vitro and in xenografts. J. Clin. Invest. *120*, 485–497.

Gual, P., Baron, V., Lequoy, V., and Van Obberghen, E. (1998). Interaction of Janus kinases JAK-1 and JAK-2 with the insulin receptor and the insulin-like growth factor-1 receptor. Endocrinology *139*, 884–893.

Haber, D.A., Gray, N.S., and Baselga, J. (2011). The evolving war on cancer. Cell *145*, 19–24.

Harrington, L.S., Findlay, G.M., Gray, A., Tolkacheva, T., Wigfield, S., Rebholz, H., Barnett, J., Leslie, N.R., Cheng, S., Shepherd, P.R., et al. (2004). The TSC1-2 tumor suppressor controls insulin-PI3K signaling via regulation of IRS proteins. J. Cell Biol. *166*, 213–223.

Harrison, C., Kiladjian, J.-J., Al-Ali, H.K., Gisslinger, H., Waltzman, R., Stalbovskaya, V., McQuitty, M., Hunter, D.S., Levy, R., Knoops, L., et al. (2012). JAK inhibition with ruxolitinib versus best available therapy for myelofibrosis. N. Engl. J. Med. *366*, 787–798.

Harry, B.L., Eckhardt, S.G., and Jimeno, A. (2012). JAK2 inhibition for the treatment of hematologic and solid malignancies. Expert Opin. Investig. Drugs *21*, 637–655.

Haruta, T., Uno, T., Kawahara, J., Takano, A., Egawa, K., Sharma, P.M., Olefsky, J.M., and Kobayashi, M. (2000). A rapamycin-sensitive pathway down-regulates insulin signaling via phosphorylation and proteasomal degradation of insulin receptor substrate-1. Mol. Endocrinol. *14*, 783–794.

Hedvat, M., Huszar, D., Herrmann, A., Gozgit, J.M., Schroeder, A., Sheehy, A., Buettner, R., Proia, D., Kowolik, C.M., Xin, H., et al. (2009). The JAK2 inhibitor AZD1480 potently blocks Stat3 signaling and oncogenesis in solid tumors. Cancer Cell *16*, 487–497.

Hudis, C.A., and Gianni, L. (2011). Triple-negative breast cancer: an unmet medical need. Oncologist *16*(*Suppl 1*), 1–11.

Jin, H., Lanning, N.J., and Carter-Su, C. (2008). JAK2, but not Src family kinases, is required for STAT, ERK, and Akt signaling in response to growth hormone in preadipocytes and hepatoma cells. Mol. Endocrinol. *22*, 1825–1841.

Le, M.N., Kohanski, R.A., Wang, L.H., and Sadowski, H.B. (2002). Dual mechanism of signal transducer and activator of transcription 5 activation by the insulin receptor. Mol. Endocrinol. *16*, 2764–2779.

Ley, R., Balmanno, K., Hadfield, K., Weston, C., and Cook, S.J. (2003). Activation of the ERK1/2 signaling pathway promotes phosphorylation and proteasome-dependent degradation of the BH3-only protein, Bim. J. Biol. Chem. *278*, 18811–18816.

Maira, S.M., Stauffer, F., Brueggen, J., Furet, P., Schnell, C., Fritsch, C., Brachmann, S., Chène, P., De Pover, A., Schoemaker, K., et al. (2008). Identification and characterization of NVP-BEZ235, a new orally available dual phosphatidylinositol 3-kinase/mammalian target of rapamycin inhibitor with potent in vivo antitumor activity. Mol. Cancer Ther. *7*, 1851–1863.

Marotta, L.L.C., Almendro, V., Marusyk, A., Shipitsin, M., Schemme, J., Walker, S.R., Bloushtain-Qimron, N., Kim, J.J., Choudhury, S.A., Maruyama, R., et al. (2011). The JAK2/STAT3 signaling pathway is required for growth of $CD44^{+}CD24^{-}$ stem cell-like breast cancer cells in human tumors. J. Clin. Invest. *121*, 2723–2735.

Muranen, T., Selfors, L.M., Worster, D.T., Iwanicki, M.P., Song, L., Morales, F.C., Gao, S., Mills, G.B., and Brugge, J.S. (2012). Inhibition of PI3K/mTOR leads to adaptive resistance in matrix-attached cancer cells. Cancer Cell *21*, 227–239.

Neve, R.M., Chin, K., Fridlyand, J., Yeh, J., Baehner, F.L., Fevr, T., Clark, L., Bayani, N., Coppe, J.P., Tong, F., et al. (2006). A collection of breast cancer cell lines for the study of functionally distinct cancer subtypes. Cancer Cell *10*, 515–527.

O'Brien, S.G., Guilhot, F., Larson, R.A., Gathmann, I., Baccarani, M., Cervantes, F., Cornelissen, J.J., Fischer, T., Hochhaus, A., Hughes, T., et al.; IRIS Investigators. (2003). Imatinib compared with interferon and low-dose cytarabine for newly diagnosed chronic-phase chronic myeloid leukemia. N. Engl. J. Med. *348*, 994–1004.

O'Reilly, K.E., Rojo, F., She, Q.B., Solit, D., Mills, G.B., Smith, D., Lane, H., Hofmann, F., Hicklin, D.J., Ludwig, D.L., et al. (2006). mTOR inhibition induces upstream receptor tyrosine kinase signaling and activates Akt. Cancer Res. *66*, 1500–1508.

Opferman, J.T. (2006). Unraveling MCL-1 degradation. Cell Death Differ. *13*, 1260–1262.

Palomero, T., Sulis, M.L., Cortina, M., Real, P.J., Barnes, K., Ciofani, M., Caparros, E., Buteau, J., Brown, K., Perkins, S.L., et al. (2007). Mutational loss of PTEN induces resistance to NOTCH1 inhibition in T-cell leukemia. Nat. Med. *13*, 1203–1210.

Parcellier, A., Tintignac, L.A., Zhuravleva, E., and Hemmings, B.A. (2008). PKB and the mitochondria: AKTing on apoptosis. Cell. Signal. *20*, 21–30.

Radimerski, T., Montagne, J., Hemmings-Mieszczak, M., and Thomas, G. (2002). Lethality of Drosophila lacking TSC tumor suppressor function rescued by reducing dS6K signaling. Genes Dev. *16*, 2627–2632.

Rodier, F., and Campisi, J. (2011). Four faces of cellular senescence. J. Cell Biol. *192*, 547–556.

Sakamoto, K., Lin, W.C., Triplett, A.A., and Wagner, K.U. (2009). Targeting janus kinase 2 in Her2/neu-expressing mammary cancer: Implications for cancer prevention and therapy. Cancer Res. *69*, 6642–6650.

Samuels, Y., Wang, Z., Bardelli, A., Silliman, N., Ptak, J., Szabo, S., Yan, H., Gazdar, A., Powell, S.M., Riggins, G.J., et al. (2004). High frequency of mutations of the PIK3CA gene in human cancers. Science *304*, 554.

Sellers, W.R. (2011). A blueprint for advancing genetics-based cancer therapy. Cell *147*, 26–31.

Serra, V., Markman, B., Scaltriti, M., Eichhorn, P.J., Valero, V., Guzman, M., Botero, M.L., Llonch, E., Atzori, F., Di Cosimo, S., et al. (2008). NVP-BEZ235, a dual PI3K/mTOR inhibitor, prevents PI3K signaling and inhibits the growth of cancer cells with activating PI3K mutations. Cancer Res. *68*, 8022–8030.

Sheppard, K., Kinross, K.M., Solomon, B., Pearson, R.B., and Phillips, W.A. (2012). Targeting PI3 kinase/AKT/mTOR signaling in cancer. Crit. Rev. Oncog. *17*, 69–95.

Solit, D.B., and Rosen, N. (2011). Resistance to BRAF inhibition in melanomas. N. Engl. J. Med. *364*, 772–774.

Traxler, P., Allegrini, P.R., Brandt, R., Brueggen, J., Cozens, R., Fabbro, D., Grosios, K., Lane, H.A., McSheehy, P., Mestan, J., et al. (2004). AEE788: a dual family epidermal growth factor receptor/ErbB2 and vascular endothelial growth factor receptor tyrosine kinase inhibitor with antitumor and antiangiogenic activity. Cancer Res. *64*, 4931–4941.

Turke, A.B., Zejnullahu, K., Wu, Y.L., Song, Y., Dias-Santagata, D., Lifshits, E., Toschi, L., Rogers, A., Mok, T., Sequist, L., et al. (2010). Preexistence and clonal selection of MET amplification in EGFR mutant NSCLC. Cancer Cell *17*, 77–88.

Waugh, D.J., and Wilson, C. (2008). The interleukin-8 pathway in cancer. Clin. Cancer Res. *14*, 6735–6741.

Wee, S., Jagani, Z., Xiang, K.X., Loo, A., Dorsch, M., Yao, Y.M., Sellers, W.R., Lengauer, C., and Stegmeier, F. (2009). PI3K pathway activation mediates resistance to MEK inhibitors in KRAS mutant cancers. Cancer Res. *69*, 4286–4293.

Xin, H., Herrmann, A., Reckamp, K., Zhang, W., Pal, S., Hedvat, M., Zhang, C., Liang, W., Scuto, A., Weng, S., et al. (2011). Antiangiogenic and antimetastatic activity of JAK inhibitor AZD1480. Cancer Res. *71*, 6601–6610.

Yamauchi, T., Ueki, K., Tobe, K., Tamemoto, H., Sekine, N., Wada, M., Honjo, M., Takahashi, M., Takahashi, T., Hirai, H., et al. (1997). Tyrosine phosphorylation of the EGF receptor by the kinase Jak2 is induced by growth hormone. Nature *390*, 91–96.

Yamauchi, T., Kaburagi, Y., Ueki, K., Tsuji, Y., Stark, G.R., Kerr, I.M., Tsushima, T., Akanuma, Y., Komuro, I., Tobe, K., et al. (1998). Growth hormone and prolactin stimulate tyrosine phosphorylation of insulin receptor substrate-1, -2, and -3, their association with p85 phosphatidylinositol 3-kinase (PI3-kinase), and concomitantly PI3-kinase activation via JAK2 kinase. J. Biol. Chem. *273*, 15719–15726.